INNOVATIVE SELECTIVE LASTER SINTERING RAPID MANUFACTURING USING NANOTECHNOLOGY

J.H. Koo[1*], L. Pilato[2], G. Wissler[2], J. Cheng[1], W. Ho[1], K. Nguyen[1], S. Lao[1], A. Cummings[1], and M. Ervin[2]

[1]The University of Texas at Austin, Dept. of Mechanical Engineering, 1 University Station C2200, Austin, TX 78712-0292

[2]KAI, Inc., 6402 Needham Lane, Austin, TX 78739-1510

[*]Corresponding author: jkoo@mail.utexas.edu

Abstract

The objective of this research is to develop an improved nylon 11 (polyamide 11) polymer with enhanced flame retardancy, thermal, and mechanical properties for selective laser sintering (SLS) rapid manufacturing (RM). A nanophase was introduced into nylon 11 via twin screw extrusion to provide improved material properties of the polymer blends. Atofina (now known as Arkema) RILSAN® nylon 11 injection molding polymer pellets was used with three types of nanoparticles: chemically modified montmorillonite (MMT) organoclays, nanosilica, and carbon nanofibers (CNF) to create nylon 11 nanocomposites. Wide angle X-ray diffraction (WAXD) and transmission electron microscopy (TEM) were used to determine the degree of dispersion. Fifteen nylon 11 nanocomposites and control nylon 11 were fabricated by injection molding. Flammability properties (using a cone calorimeter with a radiant flux of 50 kW/m^2) and mechanical properties such as tensile strength and modulus, flexural modulus, elongation at break were determined for the nylon 11 nanocomposites and compared with the baseline nylon 11. Based on flammability and mechanical material performance, five polymers including four nylon 11 nanocomposites and a control nylon 11 were cryogenically ground into fine powders for SLS RM. SLS specimens were fabricated for flammability, mechanical, and thermal properties characterization. Nylon 11-CNF nanocomposites exhibited the best overall properties for this study.

Introduction

Rapid prototyping (RP) has been embraced as a preferred tool for not only product development but, in many cases, "just-in-time manufacturing." The use of recently developed additive layered build fabrication methods of RP, particularly selective laser sintering (SLS) have the potential to facilitate true flexible manufacturing of small batch of parts "on-demand" while avoiding product-line tooling, under utilization of skilled labor and the need to maintain high overhead facilities costs.

Materials that are commonly used to fabricate polymeric SLS parts are high strength thermoplastics such as nylon (polyamide) 11 (PA11) and nylon (polyamide) 12 (PA12) as well as polycarbonate, and polystyrene. All of these polymeric materials lack flame retardancy. This is a critical safety requirement especially for the manufacture of finished products which invariably require some fire retardancy. Methods to flame retard or modify flammable thermoplastic materials to flame-retardant products [1] consists of the introduction of flame-retardant additives such as inorganic metal oxides/hydroxides (aluminum trihydrate, magnesium

hydroxide) or halogens with or without phosphorous and nitrogen containing materials. Large amounts of metal oxides (>30%) are necessary to flame retard thermoplastics and in many cases compromises some mechanical properties of the thermoplastic such as reduced toughness, melt flow, etc. Similarly use of halogens and/or phosphorous, nitrogen compounds also involves the addition of large amounts of additive(s) resulting in the release of smoke and toxic emissions when the modified thermoplastic is subjected to fire conditions.

A new procedure for developing flame-retardant thermoplastic polymers involves the use of nanotechnology whereby nanoparticles are incorporated into the thermoplastic by a melt blending process (extruder) and requires low amounts (< 7%) [2-12]. A nanophase is formed within the nanomodified thermoplastic material resulting in the formation of a nanocomposite system that forms a char barrier or insulative shield for flame retardancy. These novel nanocomposites not only exhibit improved flame retardancy but also enhanced mechanical properties such as high strength/modulus, moisture resistance, and a higher heat distortion temperature thereby meeting the objectives of improved, high strength polymer powdered materials to manufacture "net shape" replacement parts by the SLS method.

Materials Selection

Polymer Resin The polymer system is the most important component of the PA11N materials. Arekma's RILSAN® PA11 thermoplastic was selected for this study, since this is the industrial standard polymer system used by the SLS technique. RILSAN® PA11 thermoplastic [13] is a high-performance technical polymer developed by Arekma Chemicals, Inc. in 1942. Derived from a series of complex chemical operations, RILSAN® PA11 is one of the few polymers in existence produced from 'green' raw materials – castor beans. RILSAN® PA11 resin has earned a preferred material status in the most demanding applications due largely to their unique combination of thermal, physical, chemical, and mechanical properties. This results in an outstanding Cost Performance Ratio. Processing ease is another major benefit of RILSAN® PA11 resin. Supplied in powder or pellet form RILSAN® PA11 resin can be processed by injection molding, extrusion, blown film extrusion, extrusion blow molding or rotomolding. RILSAN® PA11 PCGLV pellets were used in this study. Outstanding properties of RILSAN® PA11 resin include:

- Very low specific gravity and low moisture absorption (0.9%)
- Excellent stability at high temperature
- Excellent chemical resistance and good stress crack resistance
- High dimensional stability and good creep resistance
- High abrasion resistance and low coefficient of friction

RILSAN® PA11 resin has a unique combination of properties. Their ease of processing has led designers to select them for industries as diverse as aerospace, offshore drilling, electrical cables, automotive, and pneumatic and hydraulic hose.

Polymer Nanoparticles Three types of nanoparticles were used, namely Southern Clay Products' montmorillonite (MMT) nanoclays, Degussa's nanaosilica, and Applied Sciences' carbon nanofibers (CNF). These nanoparticles are known to reinforce the polymer in the nanoscale and lead to enhancement of the dimensional stability and mechanical properties of the resulting polymer nanocomposites. To achieve these potential improvements it usually requires

excellent dispersion and some degree of exfoliation (for nanoclay). These are shown to be dependent upon a combination of proper chemical surface treatment and optimized processing.

Nanoclays Achieving exfoliation of organomontmorillonite in various continuous phases is a function of the surface treatment of the MMT clays and the mixing efficiency of the dispersing protocol. Surface treatment of MMT is classically accomplished with the exchange of inorganic counterions, e.g., sodium, etc., with quaternary ammonium ions. Two MMT nanoclays such as Southern Clay Products (a) Cloisite® 30B (a natural MMT modified with an organic modifier, MT2EtOT: methyl-tallow-bis-2-hydroxyethyl-quaternary ammonium at 90 meq/100g) [14] and (b) Cloisite® 93A (a natural MMT modified with an organic modifier M2HT: methyl-dihydrogenated tallow ammonium at 90 meq/100g clay) were used [15].

Nanosilica AEROSIL® is highly dispersed, amorphous, very pure silica that is produced by high-temperature hydrolysis of silicon tetrachloride in an oxyhydrogen gas flame [16-18]. The primary particles are spherical and free of pores. The primary particles in the flame interact to develop aggregates that join together reversibly to form agglomerates. AEROSIL® 300 is a hydrophilic fumed silica with a specific surface of 300 m^2/g manufactured by Degussa [16]. It has an average particle size of 7 nm in diameter. AEROSIL® fumed silica for rheology control is widely used in silicone rubber, coatings, plastics, printing inks, adhesives, lubricants, creams, ointment, and in toothpaste.

Carbon Nanofibers (CNF) CNF are a form of vapor-grown carbon fiber, which is a discontinuous graphitic filament produced in the gas phase from the pyrolysis of hydrocarbons [19-22]. In properties of physical size, performance improvement, and product cost, CNF complete a continuum bounded by carbon black, fullerenes, and single-wall to multi-wall carbon nanotubes on one end and continuous carbon fiber on the other end [22]. PR-19-PS CNF was used in our study.

The morphology of selective resin/nanoparticle systems was characterized using TEM and SEM analyses. These TEM images facilitated screening various formulations for desirable nano-level dispersion of the nanoclay or nanosilica or CNF within the polymer. Desirable features included higher levels of nanoclay exfoliation, nanodispersion of nanosilica, and uniform dispersion of CNF within the polymer.

Discussion of Results

Processing and Characterization of Resin/Nanoparticle Systems Processing and characterization of PA11-nanoclay, PA11-nanosilica, and PA11-carbon nanofibers are discussed in this section.

Blending Nanoclays/PA11 Polymer Chemically treated pillared clays such as Cloisite® 30B and 93A organoclays were used. The individual clay layers have been separated by alkyl ammonium ion incorporation (d spacing increased) allowing for possible intercalation of solid organic resins if the clay is melt blended with the resins. Clays were blended with the PA11 resin to intercalate and eventually exfoliate it. Twin screw extrusion mixing should enhance the exfoliation rate and the degree of exfoliation was estimated by WAXD and TEM.

A 30 mm Werner Pfleider corotating twin screw extruder was used and was configured for a wide variety of materials. Table 1 shows the two nanoclays selected at 2.5, 5, 7.5, and 10 wt% loading levels with the PA11 resin. Approximately 10 lbs of each formulation were produced. The PA11 was dried in a desiccant drier before compounding. Injection molded specimens of

each blend were prepared and examined by WAXD and TEM. Figure 1 shows the TEM micrographs of the 90% PA11:10% Cloisite® 30B. It is evident that exfoliation of Cloisite® 30B in PA11 polymer was achieved.
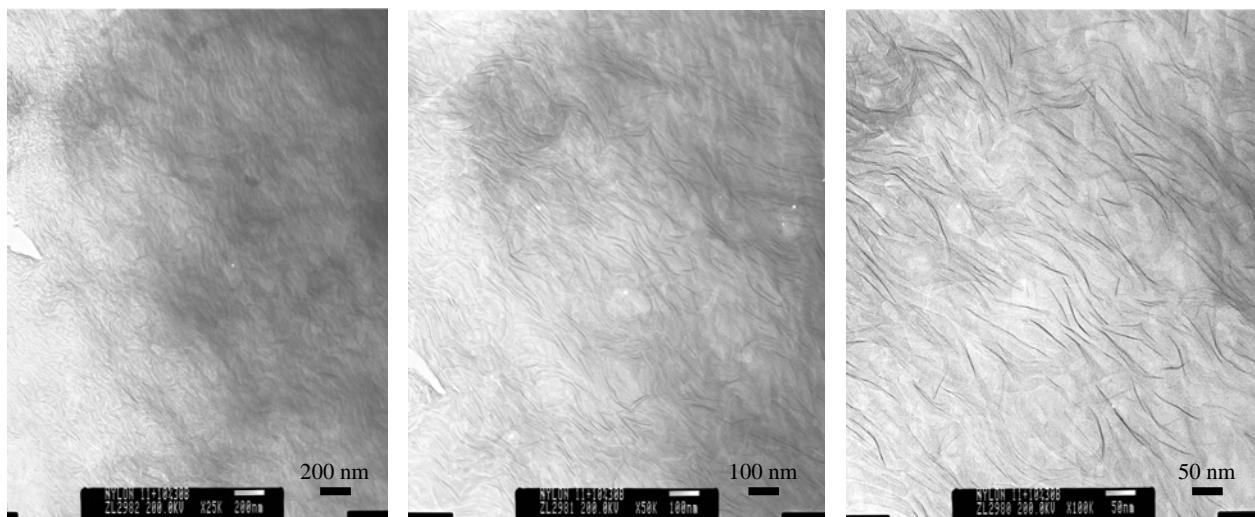

Figure 1 TEM micrographs of the 90% PA11:10% Cloisite 30B polymer showing exfoliation of nanoclay in PA11 was achieved.

Blending Carbon Nanofibers/PA11 Polymer PR-19-PS CNF is about 130 nm in diameter and several microns in length, and can be classified as MWNT. It was blended with PA11 polymer in four different loading levels via twin screw extrusion. Table 1 shows that the CNF was selected at 1, 3, 5, and 7 wt% loading levels with the PA11 resin. Approximately 10 lbs of each formulation were produced. Injection molded specimens of each blend were prepared and examined by TEM as shown in Figure 2. It is evident good dispersion of PR-19-PS CNF in PA11 was achieved.
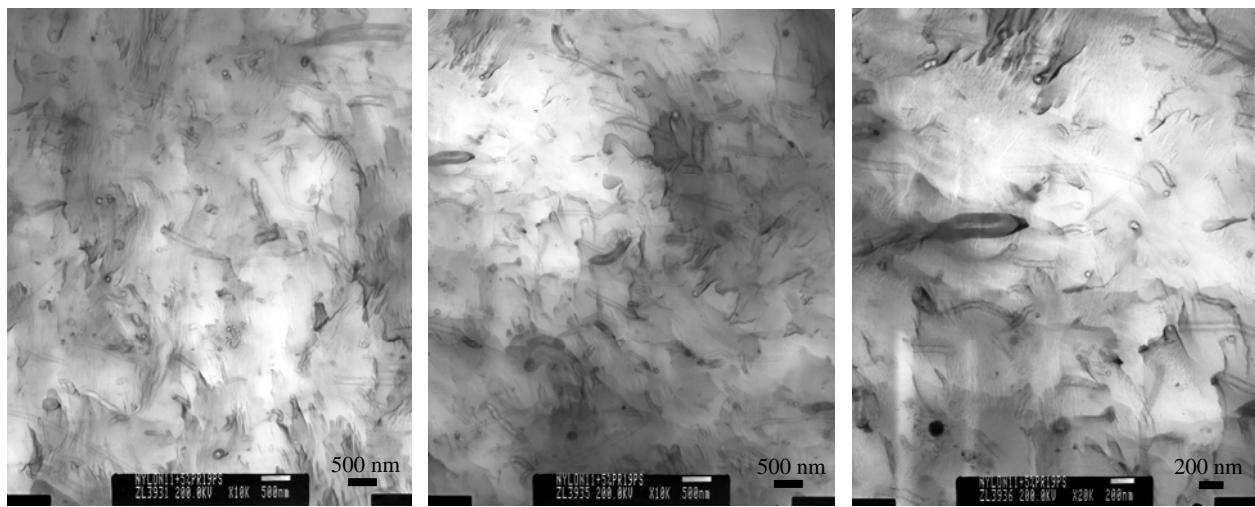

Figure 2 TEM micrographs of the 95% PA11:5% PR-19-PS polymer showing good dispersion of CNF in PA11 was achieved.

Blending Nanosilicas/PA11 Polymer Nanosilica Aerosil® 300 was blended with PA11 polymer in three different loading levels. Table 1 shows that the nanosilica was selected at 2.5, 5, and 7.5 wt% loading levels with the PA11 resin. Approximately 10 lbs of each formulation were

produced. Injection molded specimens of each blend were prepared and examined by TEM as shown in Figure 3. It is evident that nanosilicas formed very large aggregates (micron size).
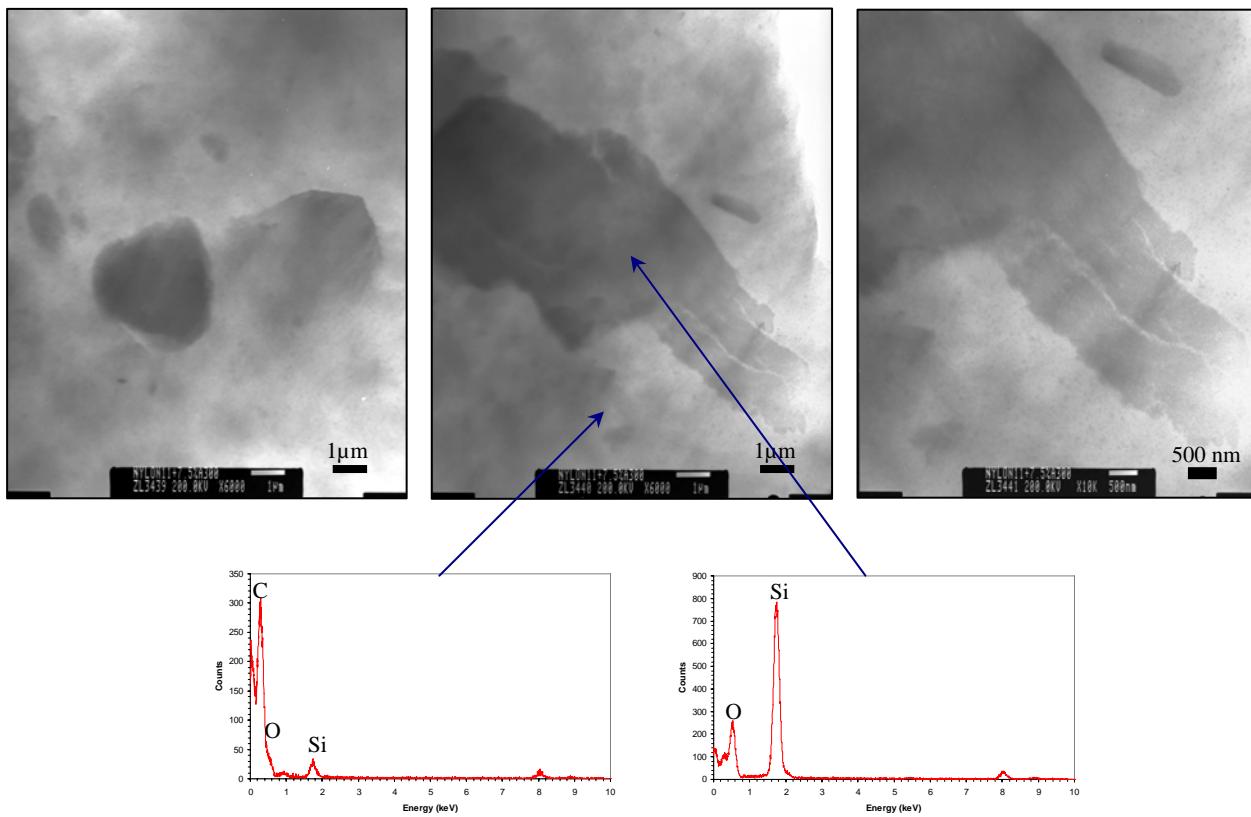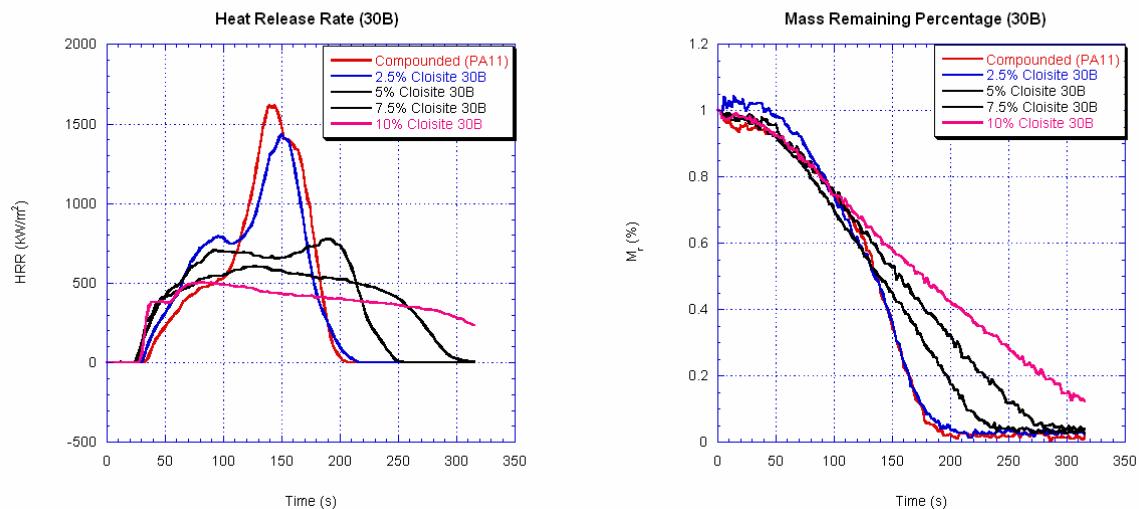

Figure 3 TEM micrographs of the 92.5% PA11:7.5% Aerosil® 300 nanosilica polymer showing very large nanosilica aggregates were formed in the PA11 polymer.

Table 1 Material Matrix for Resin/Nanoparticles

SAMPE NO.	RESIN (WT PERCENT)	NANOPARTICLES (WT PERCENT)	NANOPARTICLES TYPE
1	PA11 100%	0%	None
2	PA11 97.5%	2.5%	Cloisite® 30B
3	PA11 95%	5%	Cloisite® 30B
4	PA11 92.5%	7.5%	Cloisite® 30B
5	PA11 90%	10%	Cloisite® 30B
6	PA11 97.5%	2.5%	Cloisite® 93A
7	PA11 95%	5%	Cloisite® 93A
8	PA11 92.5%	7.5%	Cloisite® 93A
9	PA11 90%	10%	Cloisite® 93A
10	PA11 99%	1%	PR-19-PS CNF
11	PA11 97%	3%	PR-19-PS CNF
12	PA11 95%	5%	PR-19-PS CNF
13	PA11 93%	7%	PR-19-PS CNF
14	PA11 97.5%	2.5%	Aerosil® 300
15	PA11 95%	5%	Aerosil® 300
16	PA11 92.5%	7.5%	Aerosil® 300

Flammability Properties of Resin/Nanoparticle Systems The fifteen PA11 polymer blends and PA11 control in Table 1 were exposed to a radiant heat flux of 50 kW/m^2 within the Cone Calorimeter per ASTM E 1354 [23]. Each blend was tested in duplicate. The detailed average flammability properties are shown in Ref. 24. Figures 4 through 7 show the heat release rate, residual mass, carbon monoxide, and smoke extinction coefficient of the 2.5, 5, 7.5, and 10% Cloisite® 30B/97.5, 95.0, 92.5, and 90% PA11, respectively. It is evident from Table 2, the most effective nanofiller for the PA11 polymer is Cloisite® 30B. A reduction of 73% peak HRR was observed with 10% Cloisite® 30B in PA11. A reduction of the avg. HRR at 180s and mean CO yield were also exhibited. The second best nanofiller for the PA11 polymer was PR-19-PS CNF. A reduction of 71% peak PHRR was observed with 7% PR-19-PS CNF. It was followed by the Cloisite® 93A. The Aerosil® 300 nanosilica is not an effective FR nanoparticle. Table 2 summarizes the flammability and mechanical properties of all the PA11N and PA11 materials.

Figures 4 and 5 Comparison of heat release rate (left) and residue mass (right) for 2.5, 5, 7.5, 10 wt% of Cloisite® 30B PA11N at 50 kW/m^2 heat flux.

Mechanical Properties of Resin/Nanoparticle Systems Tensile strength, flexural strength, Young's modulus, and elongation at break of all the PA11N are shown in detail in Ref. 24. In summary, the 5% PR-19-PS CNF/95% PA11 polymer has the highest tensile strength. The tensile strength of all Aerosil® 300 PA11 polymer blends was lower than the control. The flexural strength of 7% PR-19-PS CNF/95 PA11 polymer is the highest among all PR-19-PS CNF formulations. Modulus was significantly increased for both PA11N containing nanoclays with 10% 30B exhibiting the highest modulus indicative of excellent dispersion/exfoliation of nanoclay in the PA11 matrix. Only low (2.5%) amounts of nanoclays showed higher elongation at break than the control. As the nanoclay was increased to 10%, a corresponding decrease in elongation was observed.
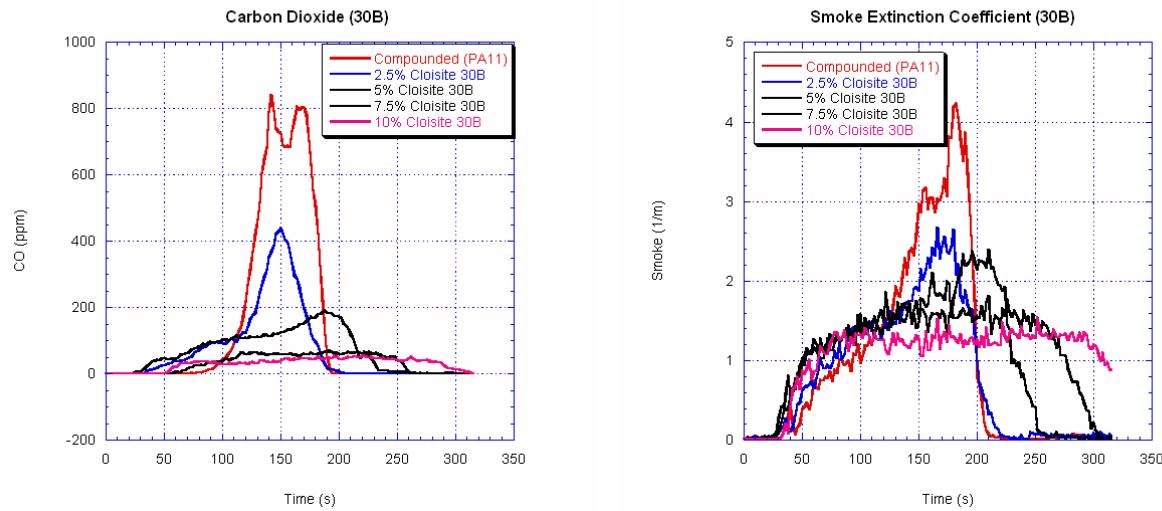
Figure 6 and 7 Comparison of carbon monoxide yield (left) and smoke extinction coefficient (right) for 2.5, 5, 7.5, 10 wt% of Cloisite® 30B PA11N at 50 kW/m^2 heat flux.

Table 2 Summary of Mechanical and Flammability Properties of the Control and Nanocomposites

Specimen ID	Pk HRR (kW/m^2)	Avg. HRR, 60s (kW/m^2)	Avg. HRR, 180s (kW/m^2)	Avg. Elong. (Strain %)	Avg. Flex. (MPa)	Avg. Tens. (MPa)
PA11 Compounded	1866	365	658	26.7	5526	7203
2.5% Cloisite® 30B	1437	510	657	52.0	6486	7499
5.0% Cloisite® 30B	784	480	621	5.4	7323	7343
7.5% Cloisite® 30B	606	441	519	3.4	7344	7344
10% Cloisite® 30B	509	430	435	1.8	6447	6549
2.5% Cloisite® 93A	1485	310	646	58.2	6179	7256
5.0% Cloisite® 93A	1349	399	661	35.1	6116	7379
7.5% Cloisite® 93A	1084	548	642	9.2	6992	6994
10% Cloisite® 93A	873	485	623	3.1	6799	6799
1.0% PR-19-PS CNF	1294	373	651	25.5	5880	7255
3.0% PR-19-PS CNF	1214	562	645	25.2	6810	7857
5.0% PR-19-PS CNF	754	497	569	23.4	7645	8294
7.0% PR-19-PS CNF	545	481	419	13.1	8249	7929
2.5% Aerosil®300	1597	419	612	8.0	6208	6208
5.0% Aerosil® 300	1560	429	612	5.3	6090	6090
7.5% Aerosil® 300	1553	429	626	4.3	5712	5712

Pk HRR   Peaked Heat Release Rate
Avg. HRR   Average Heat Release Rate, After Ignition
Avg. Elong.   Average Elongation
Avg. Flex.   Average Flexural Strength
Avg. Tens.   Average Tensile Strength

Processing and Characterization of SLS Candidates Based on flammability and mechanical properties of the injection molded PA11N candidates (Table 2), the following five materials were cryogenically ground into fine powders (about 50 µm in diameter) for SLS processing:

- Nylon 11 (control)
- Nylon 11/5% Cloisite® 30B
- Nylon 11/5% Cloisite® 93A
- Nylon 11/5 % PR-19-PS CNF
- Nylon 11/7% PR-19-PS CNF

We attempted to build SLS specimens to measure flammability, mechanical, HDT, and thermal conductivity properties using the 3D Systems Vanguard HS machine at The University of Texas at Austin/Solid Freeform Fabrication (SFF) Manufacturing Lab. The SLS process has been proven successful for nylon 11-CNF nanocomposites. It is, however, unsuccessful for nylon 11-clay nanocomposites, thus far. The observed reason for the failure is that the process is inhibited by powder mechanics. The poor powder flow for the nylon 11-clay nancomposites led to poor powder deposition and subsequent SLS processing difficulties. The difference in powder mechanics can be seen visibly: the nylon 11-clay nanocomposites flow like flour, whilst the nylon 11-CNF nanocomposites flow like grains of fine particles. Yet, there is no quantitative measurement technique in the existing SLS field to characterize powder flow behavior. This makes it very difficult to predict the processibility of a new material a priori. It is suggested that a quantitative powder mechanics characterization methodology be developed to facilitate SLS processing [25].

For the unsuccessful SLS processes, it was also suggested that a very small amount (~0.5 wt%) of fumed silica additive can be introduced to enhance powder flow and facilitate the SLS process. Further studies are needed to verify this possibility with nylon 11-clay nanocomposites.

During the processing of the nylon 11-5% CNF nanocomposites, a unique phenomenon was observed during the sintering process. Upon laser impact, the nanocomposite powder emits a consistent white light. This phenomenon was not observed in any other nylon based material, and should be investigated further. Also, the sintering of nylon 11-CNF nanocomposite appeared to produce a substantially higher content of smoke than the baseline nylon 11. An understanding of white light emission and excess smoke with nylon 11-CNF during requires additional study.

At the present, only two of the five SLS candidates were successfully fabricated and limited flammability and mechanical properties were obtained as shown in Tables 3 and 4, respectively. We were unable to translate the injection molded nylon 11 nanocomposites successes to their SLS counter parts. Preliminary data indicated density of nylon 11 plays an important role in material properties. Optimal SLS processing conditions need to be developed to fabricate denser parts to obtain enhanced material properties. Microstructural analyses of pre- and post-test PA11N specimens were conducted on injection molded and SLS specimens in order to gain fundamental understanding of material behavior [26]. Thermal conductivity data for the nylon 11-CNF are reported elsewhere [27]. Additional processing and characterization of SLS nylon 11 nanocomposites are still in progress to translate our success in the injection molded nylon 11 nanocomposites to SLS processed nylon 11 nanocomposites.

Table 3 Summary of Flammability Properties of PA11N Specimens

Sample	Peak HRR (Δ%) (kW/m^2)	Avg. HRR at 180s (Δ%) (kW/m^2)	Mean H_c (MJ/kg)	Mean SEA (m^2/kg)	Mean CO yield (kg/kg)
Nylon 11 (PA11) Injection Molded	1,866	658	33.4	201	0.025
PA11/5% PR-19-PS CNF Injection Molded	752 (60%)	569 (14%)	32.5	303	0.047
Nylon 11 (PA11) SLS	1,256	764	32.5	N/A	0.025
PA11/5% PR-19-PS CNF SLS	1,027 (18%)	775 (-1%)	32.6	N/A	0.043

Table 4 Summary of Mechanical Properties of PA11N Specimens

Sample	Tensile Yield Strength (MPa)	Flexural Strength (MPa)	Young's Modulus (GPa)	Elongation at Break (Strain %)
Nylon 11 (PA11) Injection Molded	49.7	37.6	1.36	25.1
PA11/5% PR-19-PS CNF Injection Molded	57.1	55.1	1.68	22.3
Nylon 11 (PA11) SLS	43.9	43.9	1.84	4.6
PA11/5% PR-19-PS CNF SLS	In progress	In progress	In progress	In progress

Summary and Conclusions

The nylon 11 (polyamide 11 - PA11) polymer and three types of nanoparticles (MMT nanoclay, nanosilica, and CNF) were selected for this study. A total of 15 polymer blends were compounded via twin screw extrusion and compared with the control PA11. The TEM analysis was used to study the morphology of all the polymer blends. Physical properties such as specific gravity and hardness were measured. Mechanical properties such as tensile strength, flexural strength, elongation at break, and Young's modulus were measured. Thermal properties such as thermal conductivity were measured [27]. Flammability properties were measured by Cone Calorimeter at a radiant heat flux of 50 kW/m^2. Five polymers were cryogenically ground into fine powders (50 µm in diameter) for SLS processing. Mechanical, flammability, and thermal properties were characterized for these SLS specimens.

The following conclusions were drawn from this study:

1. The TEM analysis has been demonstrated as an effective and efficient tool to characterize and screen candidates based on their degree of dispersion.
2. The peak release rate of the injection molded PA11-nanoclay polymers decreases as the amount of nanoclay increases with PA11-10 % Cloisite 30B with a PHRR of 509 kW/m^2 a reduction of 73% as compared with PA11 with a PHRR of 1,866 kW/m^2.

3. The peak release of injected molded PA11-CNF polymers also decreases as the amount of CNF increases with PA11-7% PR-19-PS CNF with a PHRR of 545 kW/m^2 reduction of 71%.
4. Cloisite® 30B has better flammability properties than Cloisite® 93A.
5. Nanosilica does not enhance the flammability and mechanical properties of PA11 due to poor dispersion of nanosilica in the PA11 polymer.
6. For the injection molded specimens, subtle features of using nanoclay or CNF as nanomaterial in PA11N indicate that CNF provided the highest tensile yield strength as well as flexural strength whereas the nanoclays provided enhanced modulus with increasing amount of nanoclay. The benefit of improved elongation at break occurred only at low amounts of nanoclay (2.5%) with elongation decreasing as the amount of nanoclay was increased above 2.5%. Little or no benefit was observed with nanosilica and is attributable to poor dispersion.
7. The technical objective of transforming nanomodified nylon 11 (PA11/5% PR-19-PS CNF) by SLS into an SLS component for characterization for flammability behavior (Cone Calorimeter) and mechanical properties was achieved.
8. Only two (nylon 11 baseline and nylon 11/5% PR-19-PS CNF) of the five planned SLS candidates were successfully fabricated and limited mechanical and flammability properties were determined. We were unable to translate the injection molded nylon 11 nanocomposites successes to their SLS counter parts. Preliminary data indicated density of nylon 11 plays an important role in flammability and mechanical properties. Optimal SLS processing conditions are needed to identify the procedure to fabricate denser parts to enhance material properties.
9. Powder mechanics and powder flow behavior characterization are suggested as assisting in obtaining optimum SLS components.
10. Microstructure analyses of pre- and post-test PA11N specimens were conducted on injection molded and SLS specimens to gain fundamental understanding of material behavior. These results are reported elsewhere [26].
11. Additional processing and characterization of SLS nylon 11 nanocomposites are reported elsewhere [25] and indicate our success in the injection molded nylon 11 nanocomposites to SLS processed nylon 11 nanocomposites.

References

1. *Fire and Polymers III. Materials and Solutions for Hazard Prevention*, G.N. Nelson and C.A. Wilke, Ed., American Chemical Society, Washington, D.C., 2001.
2. E. Giannelis, *Adv. Mater.* 8, 29 (1996).
3. J.W. Gilman, T. Kashiwagi, *SAMPE J.,* 33 (4), 40 (1997).
4. J.W. Gilman, *Appl. Clay. Sci.* 15, 31 (1999).
5. J. Zhu, A.B. Morgan, J. Lamelas, C.A. Wilke, *Chem. Mater.* 13, 3774 (2001).
6. M. Zanetti, G. Camino, R. Mulhaupt, *Polym. Degrad. Stabil.* 74, 413 (2001).
7. J.W. Gilman, C.L. Jackson, A.B. Morgan, R. Harris, Jr., E. Manias, E. P. Giannelis, M. Wuthernow, D. Hilton, S.H. Phillips, *Chem. Mater.* 12, 1866 (2000).
8. T. Kashiwagi, E. Grulke, J. Hilding, R. Harris, W. Awad, J. Douglas, *Macromol. Rapid Commun.*, 23, 761 (2002).
9. J.H. Koo *et al.*, *Proc. SAMPE 2003*, SAMPE, Covina, CA, 2003, p. 954.

10. F. Yang, R.A. Yngard, G.L. Nelson, "Nanocomposites 2002," San Diego, CA, Sept 23-5, 2002.
11. T. Kashiwagi *et al.*, "Nanocomposites 2002," San Diego, CA, Sept 23-5, 2002.
12. A.D. Pool and H.T. Hahn, *Proc. SAMPE 2003*, SAMPE, Covina, CA, 2003.
13. RILSAN® polyamide 11 technical data sheet, Arekma Chemicals, Inc.
14. B. Powell, Southern Clay Products, Gonzales, TX, personal communication, 10/2003 and Cloisite® 30B technical data sheet.
15. D. Hunter, Southern Clay Product, Gonzales, TX, personal communication, 10/2003 and Cloisite® 93A technical data sheet, Gonzales, TX.
16. Technical Bulletin AEROSIL® No. 27, Degussa AG, D-63403 Hanau-Wolfgang, Germany, 10/2001.
17. AEROSIL® R805 technical data sheet, Degussa AG, D-63403 Hanau-Wolfgang, Germany.
18. AEROSIL® R202 technical data sheet, Degussa AG, D-63403 Hanau-Wolfgang, Germany.
19. G.G. Tibbetts, *J. Crystal Growth* 1984; 66:632.
20. M.L. Lake, J-M. Ting. In *Carbon Materials for Advanced Technologies*, T.D. Burchell, Ed., Pergamon, Oxford: England, 1999.
21. M.L. Lake, manuscript from Applied Sciences, Inc., Cedarville, OH, 11/2002.
22. B. Maruyama and K. Alam, *SAMPE J.*, 38 (3), 59 (2002).
23. Standard Test Method for Heat and Visible Smoke Release Rates for Materials and Products Using an Oxygen Consumption Calorimeter, ASTM E 1354, ASTM, Philadelphia, PA.
24. J.H. Koo, L. Pilato, G. Wissler, and Z.P. Luo, "Flammability and Mechanical Properties of Nylon 11 Nanocomposites," *Proc. SAMPE 2005*, SAMPE, Covina, 2005.
25. J. Cheng, S. Lao, K. Nguyen, D. Ho, T. Cummings, and J.H. Koo, "SLS Processing of Nylon 11 Nanocomposites," presented at the 17th Solid Freeform Fabrication Symposium, The University of Texas at Austin, Austin, TX, Aug. 2005.
26. S. Lao, W. Ho, K. Nguyen, J. Cheng, and J.H. Koo, "Microstructural Analyses of Nylon 11 Nanocomposites," accepted for presenting at the *37th International SAMPE Technical Conference*, Seattle, WA, Oct. 31 – Nov.3, 2005.
27. A. Cummings, L. Shi, and J.H. Koo, "Thermal Conductivity Measurements of Nylon 11-Carbon Nanofiber Nanocomposites," *Proc. of IMECE2005 (2005 ASME International Mechanical Engineering Congress & Exposition)*, Orlando, FL, Nov. 5-11, 2005.